

This is an Open Access document downloaded from ORCA, Cardiff University's institutional repository:<https://orca.cardiff.ac.uk/id/eprint/109372/>

This is the author's version of a work that was submitted to / accepted for publication.

Citation for final published version:

Nishio Ayre, Wayne , Melling, Genevieve , Cuveillier, Camille, Natarajan, Madhan, Roberts, Jessica L., Marsh, Lucy L., Lynch, Christopher D., Maillard, Jean-Yves , Denyer, Stephen P. and Sloan, Alastair J. 2018. *Enterococcus faecalis* demonstrates pathogenicity through increased attachment in an ex vivo polymicrobial pulpal infection. *Infection and Immunity* 86 (5) , e00871-17. 10.1128/IAI.00871-17

Publishers page: <http://doi.org/10.1128/IAI.00871-17>

Please note:

Changes made as a result of publishing processes such as copy-editing, formatting and page numbers may not be reflected in this version. For the definitive version of this publication, please refer to the published source. You are advised to consult the publisher's version if you wish to cite this paper.

This version is being made available in accordance with publisher policies. See <http://orca.cf.ac.uk/policies.html> for usage policies. Copyright and moral rights for publications made available in ORCA are retained by the copyright holders.



1 ***Enterococcus faecalis* demonstrates pathogenicity through increased**  
2 **attachment in an *ex vivo* polymicrobial pulpal infection**

3

4 Wayne Nishio Ayre,<sup>a#</sup> Genevieve Melling,<sup>a</sup> Camille Cuveillier,<sup>a</sup> Madhan Natarajan,<sup>a</sup>  
5 Jessica L. Roberts,<sup>a+</sup> Lucy L. Marsh,<sup>a</sup> Christopher D. Lynch,<sup>b</sup> Jean-Yves Maillard,<sup>c</sup>  
6 Stephen P Denyer,<sup>d</sup> Alastair J. Sloan<sup>a</sup>

7

8 <sup>a</sup> School of Dentistry, Cardiff University, Cardiff, UK.

9 <sup>b</sup> University Dental School & Hospital, University College Cork, Cork, Ireland

10 <sup>c</sup> School of Pharmacy and Pharmaceutical Sciences, Cardiff University, Cardiff, UK

11 <sup>d</sup> School of Pharmacy and Biomolecular Sciences, University of Brighton, Brighton,  
12 UK

13

14 Running Head: *E. faecalis* pulpal pathogenicity and attachment

15

16 #Address correspondence to Wayne Nishio Ayre, ayrewn@cardiff.ac.uk

17 +Present address: North Wales Centre for Primary Care Research, Bangor

18 University, Bangor, UK

19

20

21

22

23

24

25

26 **Abstract**

27 This study investigated the host response to a polymicrobial pulpal infection  
28 consisting of *Streptococcus anginosus* and *Enterococcus faecalis*, bacteria  
29 commonly implicated in dental abscesses and endodontic failure, using a validated  
30 *ex vivo* rat tooth model. Tooth slices were inoculated with planktonic cultures of *S.*  
31 *anginosus* or *E. faecalis* alone or in co-culture at ratios of 50:50 and 90:10 *S.*  
32 *anginosus* to *E. faecalis*. Attachment was semi-quantified by measuring area  
33 covered by fluorescently labelled bacteria. Host response was established by viable  
34 histological cell counts and inflammatory response using RT-qPCR and  
35 immunohistochemistry. A significant reduction in cell viability was observed for single  
36 and polymicrobial infections, with no significant differences between infection types  
37 ( $\approx 2000$  cells/mm<sup>2</sup> for infected pulps compared to  $\approx 4000$  cells/mm<sup>2</sup> for uninfected  
38 pulps). *E. faecalis* demonstrated significantly higher levels of attachment (6.5%)  
39 compared to *S. anginosus* alone (2.3%) and mixed species infections (3.4% for  
40 50:50 and 2.3% for 90:10), with a remarkable affinity to the pulpal vasculature.  
41 Infections with *E. faecalis* demonstrated the greatest increase in TNF- $\alpha$  (47.1 fold for  
42 *E. faecalis*, 14.6 fold for *S. anginosus*, 60.1 fold for 50:50 and 25.0 fold for 90:10)  
43 and IL-1 $\beta$  expression (54.8 fold for *E. faecalis*, 8.8 fold for *S. anginosus*, 54.5 fold for  
44 50:50 and 39.9 fold for 90:10) when compared to uninfected samples.  
45 Immunohistochemistry confirmed this with the majority of inflammation localised to  
46 the pulpal vasculature and odontoblast regions. Interestingly, *E. faecalis* supernatant  
47 and heat killed *E. faecalis* treatment was unable to induce the same inflammatory  
48 response, suggesting *E. faecalis* pathogenicity in pulpitis is linked to its greater ability  
49 to attach to the pulpal vasculature.

50

## 51 **Introduction**

52           The dental pulp is a complex environment composed of soft connective tissue,  
53 nerves, blood vessels and a variety of cells, such as dental pulp stem cells,  
54 fibroblasts and odontoblasts (1). When the pulp becomes inflamed in response to  
55 bacterial infection or other stimuli, this is known as pulpitis. Early stages are  
56 considered “reversible” and treatment involves removal of the stimulus, such as  
57 carious lesions, in order to maintain pulp vitality. If untreated however, the microbial  
58 invasion may progress into the deeper dentin and subsequently the pulpal chamber  
59 resulting in severe tissue degradation and necrosis. This condition, known as  
60 “irreversible pulpitis”, requires a challenging and difficult endodontic or root canal  
61 treatment, which involves the removal of the pulp and obturation with an inert  
62 material. The success rate of root canal treatments is highly variable, ranging from  
63 31% to 96% depending on clinical considerations (2) and studies across a range of  
64 countries have shown a high percentage (up to 67.9%) of patients who have  
65 undergone this treatment subsequently develop apical periodontitis (3, 4). An  
66 alternative endodontic treatment is vital pulpotomy, which involves removal of the  
67 coronal pulp, leaving the radicular pulp vital and free of any pathological alterations  
68 (5). Although this procedure is thought to require shorter appointment times and can  
69 be accomplished in one visit, the efficacy of this technique is debated with success  
70 rates of clinical studies ranging from 70% to 96% (6). Accurate models to better  
71 understand the process of pulpal infection and to test the efficacy of novel  
72 therapeutics will aid in the development of more effective vital pulp treatments. *In*  
73 *vitro* monolayer cell culture models lack the complexity of the pulpal matrix, whilst *in*  
74 *vivo* studies suffer from systemic factors, high costs and ethical considerations. To  
75 overcome these limitations, Roberts et al. (7) developed an *ex vivo* co-culture

76 system to model pulpal infections on rat tooth slices. This study focused  
77 predominantly on the *Streptococcus anginosus* group (SAG), consisting of *S.*  
78 *anginosus*, *S. constellatus* and *S. intermedius*, Gram-positive cocci which are part of  
79 the body's commensal flora. This group are known to be primary colonisers of the  
80 oral cavity due to their ability to attach to the salivary pellicle and other oral bacteria  
81 (8). They are considered opportunistic pathogens and have been reported to form  
82 dental abscesses (9). The study by Roberts et al. demonstrated a significant  
83 reduction in viable pulp cells, an increase in cytokine expression and bacterial  
84 attachment over 24 hours as a result of *S. anginosus* infections (7).

85         Although Roberts et al. demonstrated invasion of the dental pulp by *S.*  
86 *anginosus* group species, the number of microbial species encountered in the oral  
87 cavity is far more diverse, with studies identifying between 100 to 300 different  
88 species from different regions of the oral cavity of healthy individuals (10). It is  
89 therefore unsurprising that complex mixed species microbiomes are often detected  
90 in cases of pulpitis (11). As lesions progress into the tooth, a shift in microbial  
91 species has been well documented due to environmental and nutritional changes  
92 (12). Of particular interest is the *Enterococcus faecalis* species, a Gram-positive  
93 facultative anaerobic coccus, also part of the normal human commensal flora (13). *E.*  
94 *faecalis* has been shown to be pathogenic, particularly in endodontic failure (14) with  
95 prevalence in such infections ranging from 24% up to 77% (15). Although highly  
96 implicated in persistent endodontic failure, molecular studies have recently revealed  
97 this species is frequently present in necrotic pulps, highlighting its potential role in  
98 late-stage pulpitis (16, 17).

99         This study aims to use a validated *ex vivo* co-culture model to quantify and  
100 better understand the host tissue response to mixed species pulpal infections

101 caused by *S. anginosus* and *E. faecalis*. Understanding the mechanism of complex  
102 pulpal infections and the host inflammatory response may elucidate potential targets  
103 for more effective vital pulp therapies.

104

## 105 **Results**

106 *Mixed species culture does not significantly influence S. anginosus and E. faecalis*  
107 *growth rate.*

108 Growth characteristics in a simple mixed species planktonic broth culture were  
109 investigated to ensure potential competitive growth between *S. anginosus* and *E.*  
110 *faecalis* would not influence the *ex vivo* experiments investigating host tissue  
111 response.

112 Clinical isolates of *S. anginosus* and *E. faecalis* species were selected from the  
113 culture collection of the Oral Microbiology Unit, School of Dentistry at Cardiff  
114 University. Species identity was confirmed by standard microbial identification tests  
115 and 16S rRNA sequencing as described in the methods and supplemental materials  
116 (Fig. S1 and S2).

117 Fig. 1 shows the planktonic growth curves for *S. anginosus* and *E. faecalis* alone  
118 and in combination at ratios of 50:50 and 90:10 respectively over 24 hours in BHI. *E.*  
119 *faecalis* reached mid-log phase earlier than *S. anginosus* (8 hours for *E. faecalis*  
120 compared to 10 hours for *S. anginosus*). When cultured at a ratio of 50:50 however,  
121 *S. anginosus* reached mid-log at a similar time to *E. faecalis* (10 hours). When the  
122 bacteria were cultured at an *S. anginosus* to *E. faecalis* ratio of 90:10, *S. anginosus*  
123 reached mid-log at approximately 8 hours and *E. faecalis* at approximately 12 hours.  
124 Growth rate calculations during the log phase demonstrated no significant

125 differences between *E. faecalis* and *S. anginosus* under all culture conditions  
126 ( $p > 0.05$ , Table 1).

127

128 *E. faecalis* demonstrates greater levels of attachment to dental pulp than *S.*  
129 *anginosus* at 24 hours, with particular affinity to the pulpal vasculature.

130 To assess differences in bacterial attachment to the dental pulp, the *ex vivo* rat  
131 tooth model was infected with planktonic cultures of *S. anginosus* and *E. faecalis*  
132 individually or as mixed species infections. Gram staining and fluorescent labelling  
133 of bacteria were undertaken to localise and semi-quantify bacterial attachment.

134 High levels of bacterial attachment to the pulp were detected for tooth slices  
135 incubated with *E. faecalis* (Fig. 2A) and mixed species of *S. anginosus* and *E.*  
136 *faecalis* (Fig. 2B to 2C). Attachment was predominantly observed in intercellular  
137 spaces within the pulpal matrix and around the pulpal vasculature. Bacteria were  
138 also observed attached to soft tissue surrounding the tooth and within dentinal  
139 tubules (Fig. 2D and 2E). Attachment of bacteria was not detected using Gram  
140 staining on tooth slices incubated with *S. anginosus* alone.

141 Control samples demonstrated low levels of background fluorescence (Fig. 3A).  
142 Infections consisting of *E. faecalis* alone had the greatest fluorescent signal, in  
143 particular centred near the pulpal vasculature (Fig. 3B). *S. anginosus* demonstrated  
144 low bacterial attachment, spread evenly across the pulp (Fig. 3C). When combining  
145 *E. faecalis* and *S. anginosus*, higher levels of attachment were observed compared  
146 to *S. anginosus* alone (Fig. 3D to 3E), with attachment again localised predominantly  
147 to the pulpal vasculature. When the percentage bacterial coverage was semi-  
148 quantified (Fig. 3F), the single species *E. faecalis* infection had significantly higher  
149 levels of bacterial attachment when compared to *S. anginosus* alone (approximately

150 6.5% compared to 2%,  $p=0.00021$ ) and the mixed species infections (50:50,  
151  $p=0.0235$  and 90:10,  $p=0.0032$ ).

152

153 *S. anginosus* and *E. faecalis* infections significantly reduce pulp cell viability with *E.*  
154 *faecalis* infections inducing a significantly greater inflammatory response.

155 To establish the dental pulp host response to *S. anginosus* and *E. faecalis*  
156 infections alone and as mixed species infections, histomorphometric analysis was  
157 performed alongside RT-qPCR and immunohistochemistry for TNF- $\alpha$  and IL-1 $\beta$   
158 expression.

159 Histological cell counts of the infected tooth sections demonstrated a significant  
160 reduction ( $p\leq 0.05$ ) in viable cells due to infection by both *E. faecalis* and *S.*  
161 *anginosus* alone and in combination (Fig. 4A). There were no significant differences  
162 in cell numbers between single species infections and multi-species infections.

163 All infected samples had significantly higher pro-inflammatory cytokine  
164 expression, tumour necrosis factor alpha (TNF- $\alpha$ , Fig. 4B) and interleukin 1 beta (IL-  
165 1 $\beta$ , Fig. 4C), when compared to the control samples ( $p\leq 0.05$ ). The single species  
166 infection of *E. faecalis* resulted in significantly higher levels of TNF- $\alpha$  and IL-1 $\beta$   
167 expression when compared to *S. anginosus* ( $p=0.0276$  and  $p=0.0234$  for TNF- $\alpha$  and  
168 IL-1 $\beta$  respectively). Combining *E. faecalis* and *S. anginosus* together did not result  
169 in a significantly higher inflammatory response from the pulp when compared to *E.*  
170 *faecalis* alone (for TNF- $\alpha$   $p=0.493$  and  $p=0.096$  for 50:50 and 90:10 respectively and  
171 for IL-1 $\beta$   $p=0.988$  and  $p=0.400$  for 50:50 and 90:10 respectively).

172 Negative controls replacing the primary TNF- $\alpha$  antibody with a nonimmune  
173 immunoglobulin G control showed no immunopositivity (Fig. S3). Similarly, primary  
174 exclusion controls were negative for staining, indicating specific binding of the



175 secondary antibody (Fig. S3). Control samples demonstrated low expression of  
176 TNF- $\alpha$  and interestingly *S. anginosus* alone did not induce a high TNF- $\alpha$  response  
177 (Fig. 4D). Samples incubated with *E. faecalis* alone or in combination with *S.*  
178 *anginosus* had the most pronounced staining, both within the pulp (around the  
179 vasculature) and the odontoblast layer. The level of TNF- $\alpha$  staining in these samples  
180 was similar to those encountered in the rat lung positive control (Fig. S3).

181       Immunohistochemistry staining for IL-1 $\beta$ , showed no positive signal for IgG  
182 and primary exclusion controls (Fig. S3). Similar to the TNF- $\alpha$   
183 immunohistochemistry, the control sample and the sample incubated with *S.*  
184 *anginosus* alone had few positively stained cells, whilst samples incubated with *E.*  
185 *faecalis* alone and in combination with *S. anginosus* had more positively stained cells  
186 (Fig. 4D). Although the level of staining was not as pronounced as observed with  
187 TNF- $\alpha$ , the positive cells were again located adjacent to the pulpal vasculature and  
188 similar in staining to the positive lung control (Fig. S3).

189

190 *Greater host inflammatory response to E. faecalis is not due to differences in water*  
191 *soluble cell wall proteins or culture supernatants.*

192       To establish whether the increased host inflammatory response to *E. faecalis*  
193 was due to specific water soluble cell proteins or components of the culture  
194 supernatant, SDS-PAGE was performed to identify proteins in water soluble cell wall  
195 proteins and culture supernatants. Similarly, heat killed *E. faecalis* and *E. faecalis*  
196 supernatant was used to stimulate the pulp in order to assess the host response.

197       Few differences were observed between the water soluble cell wall proteins of *S.*  
198 *anginosus* and *E. faecalis* when cultured alone and in combination with each other  
199 (Fig. S4A). In terms of the culture supernatant, there was one band at approximately

200 35kDa observed with the *E. faecalis* cultures that was not observed with *S.*  
201 *anginosus* (Fig. S4B).

202 When culturing the rat tooth slices with the *E. faecalis* supernatant or the heat  
203 killed *E. faecalis*, no significant differences were observed in TNF- $\alpha$  expression when  
204 compared to the untreated controls (Fig. 5A,  $p=0.196$  and  $p=0.152$  for supernatant  
205 and heat killed *E. faecalis* respectively). A significant increase was observed in IL-1 $\beta$   
206 expression for the tooth slices cultured with heat killed *E. faecalis* when compared to  
207 the untreated controls (Fig. 5B,  $p=0.041$ ) but not for *E. faecalis* supernatant  
208 ( $p=0.148$ ).

209 The negative controls (IgG control and primary exclusion) and the control sample  
210 for the TNF- $\alpha$  immunohistochemistry did not show staining (Fig. S5). The tooth  
211 slices incubated with *E. faecalis* supernatant had few cells stained positive for TNF- $\alpha$ ,  
212 the majority of which was concentrated at the pulpal vasculature and odontoblast  
213 layer (Fig. 5C). Similarly, the heat-killed *E. faecalis* had few cells expressing TNF- $\alpha$   
214 (Fig. 5C), whilst the lung positive control stained positive for TNF- $\alpha$  (Fig. S5).

215 The IgG control, the primary exclusion control and the untreated sample (Fig. S5)  
216 did not stain positive for IL-1 $\beta$ . Fewer cells were positive for IL-1 $\beta$  than TNF- $\alpha$  (Fig.  
217 5C). Samples treated with *E. faecalis* supernatant showed some cells stained  
218 positive within the pulpal vasculature, whilst heat-killed *E. faecalis* showed few  
219 positively stained cells. The positive lung control demonstrated cells stained positive  
220 for IL-1 $\beta$  expression (Fig. S5).

221

## 222 Discussion

223 This study has successfully employed an existing *ex vivo* rat tooth infection  
224 model to study the effect of mixed species *E. faecalis* and *S. anginosus* pulpal  
225 infections on cell viability, bacterial attachment and host inflammatory response.

226 By studying simple planktonic growth kinetics, it was established that *E. faecalis*  
227 caused the *S. anginosus* bacteria to reach log phase at a more rapid rate. This  
228 concept of polymicrobial synergy has been highlighted in recent work, which  
229 investigated metabolite cross-feeding, whereby metabolic end-products produced by  
230 one bacterium are consumed by a second community member (18-20). In particular,  
231 this has been demonstrated for a similar oral pathogen, *Streptococcus gordonii*.  
232 Lactate produced by *S. gordonii* as the primary metabolite during catabolism of  
233 carbohydrates was found to support the growth of *Aggregatibacter*  
234 *actinomycetemcomitans* (20). Interestingly, in a study using a primate model, the  
235 addition of *E. faecalis* to a four-strain mixed species culture resulted in higher levels  
236 of survival of all four bacteria than in the absence of *E. faecalis* (21). Another  
237 mechanism of coordinating activities and communicating between microbial species  
238 is quorum sensing, which has been shown to occur between different groups of  
239 Streptococci (22). Although the rate of growth during the log phase was not altered  
240 during mixed species planktonic culture in this study, it is important to appreciate that  
241 under mixed species biofilm conditions, alterations in growth are likely to occur.

242 The mixed species infection did not result in higher levels of bacterial attachment  
243 when compared to *E. faecalis* alone. The data suggests that *E. faecalis* is capable  
244 of attaching to the dental pulp to a greater extent than *S. anginosus*, with a particular  
245 affinity to the pulpal vasculature. This was not attributed to a more rapid rate of  
246 growth or higher number of bacteria as a similar number of *S. anginosus* was

247 counted after 24 hours in planktonic broth culture. Similarly in the mixed species  
248 culture where *S. anginosus* achieved log phase at an earlier time point, attachment  
249 was not as high when compared to *E. faecalis* alone. The increased attachment  
250 may therefore be due to differences between the species in terms of motility, sensing  
251 or cell surface adhesins. *E. faecalis* and *S. anginosus* are classified as groups D  
252 and F respectively using Lancefield grouping (23), a method of grouping based on  
253 the carbohydrate antigens on the cell wall. These differences in surface  
254 carbohydrates could mediate changes in attachment to epithelial cells as  
255 demonstrated by Guzman et al. (24). A review by Fisher and Phillips (25)  
256 highlighted *E. faecalis* specific cell wall components which play a vital role in  
257 pathogenic adhesion. Aggregation substance (Agg) increases hydrophobicity and  
258 aids adhesion to eukaryotic and prokaryote surfaces and also encourages the  
259 formation of mixed-species biofilm through adherence to other bacteria.  
260 Extracellular surface protein (ESP) promotes adhesion, antibiotic resistance and  
261 biofilm formation. Adhesin to collagen of *E. faecalis* (ACE) is a collagen binding  
262 protein belonging to the microbial surface components recognizing adhesive matrix  
263 molecules (MSCRAMM) family. ACE plays a role in the pathogenesis of  
264 endocarditis and *E. faecalis* mutants which do not express ACE have been shown to  
265 have significantly reduced attachment to collagens type I and IV but not fibrinogen  
266 (26, 27). Whilst *S. anginosus* has been shown to adhere to the extracellular matrix  
267 components fibronectin, fibrinogen and laminin, binding to collagens type I and IV  
268 was much less prominent (28). This is of particular interest in explaining differences  
269 in pulpal adherence and the affinity of *E. faecalis* to localise near the pulpal  
270 vasculature, as collagen fibres are often found in higher density around blood  
271 vessels and nerves (29).

272 Although the level of cell death was the same between the groups tested,  
273 infections consisting of *E. faecalis* alone produced a greater inflammatory response  
274 when compared to *S. anginosus* and mixed species infections. This increase in  
275 inflammation was not due to supernatant or water-soluble cell wall virulence factors  
276 of *E. faecalis* as treatment of the dental pulp with these isolated factors did not yield  
277 high levels of TNF- $\alpha$  and IL-1 $\beta$  expression both at gene and protein level. Basic  
278 analysis of supernatant and water soluble cell-wall proteins by SDS-PAGE showed  
279 similar bands, however this may be due to the absence of serum or collagen  
280 (present in the co-culture model) which has been shown to influence virulence factor  
281 production, such as ACE (27). These results indicate the pulpal inflammation  
282 caused by *E. faecalis* is likely due to the higher levels of attachment to the dental  
283 pulp. Similar pathogenic traits have been established for *E. faecalis* in urinary tract  
284 infections and endocarditis (30). Increased attachment to the dental pulp would  
285 allow direct contact between cells and cell wall components such as lipoteichoic acid  
286 (LTA), which induces activation of cluster of differentiation 14 (CD-14) and toll-like  
287 receptor 2 (TLR-2) (31). An *in vivo* study, which infected canine pulp with  
288 lipopolysaccharides (LPS) from *Escherichia coli* and lipoteichoic acid (LTA) from *E.*  
289 *faecalis*, demonstrated LTA treatment led to pulp destruction, albeit to a lesser extent  
290 than LPA (32). *In vitro* studies investigating macrophage responses to *E. faecalis*  
291 LTA found that TNF- $\alpha$  expression was significantly increased in a dose-dependent  
292 manner (33), with one study attributing it to the NF- $\kappa$ B and p38 MAPK signalling  
293 pathways (34). These studies however were performed using monolayer cultures,  
294 allowing easy access for LTA to activate toll-like receptors, whereas the presence  
295 extracellular matrix would limit penetration of virulence factors into the dental pulp *in*  
296 *vivo*. Furthermore macrophages are normally present as monocytes in normal

297 healthy pulp and require a stimulus to become activated (35). Studies using  
298 immunohistochemistry have shown these monocytes as well as dendritic cells to be  
299 located predominantly around blood vessels, with few distributed throughout the pulp  
300 (36, 37).

301 High levels of TNF- $\alpha$  expression were also observed in the odontoblast region  
302 using immunohistochemistry. Due to its anatomical location, odontoblasts are the  
303 first cells to encounter foreign antigens either through infiltration of virulence factors  
304 through dentinal tubules or the breakdown of enamel and dentine. Through Gram  
305 staining in this study, *E. faecalis* was observed within the dentinal tubules of the  
306 infected tooth slices. This phenomenon has been previously reported in human  
307 teeth (38). Odontoblasts, which line the dentine, have been shown to express TLRs  
308 and play a role in the pulp's immune response, in particular to bacterial exotoxins  
309 (39-41). This explains the high inflammatory response observed for both infections  
310 and supernatant treatments when assessed using immunohistochemistry. Cytokine  
311 gene expression using RT-qPCR however did not demonstrate higher levels when  
312 treating the dental pulp with supernatants or heat killed bacteria. This may be  
313 attributed to the fact that the methods employed for pulp extraction would be unlikely  
314 to fully remove the odontoblast cells.

315 Although the host response to a mixed species infection consisting of *S.*  
316 *anginosus* and *E. faecalis* has been established and the potential pathogenicity of *E.*  
317 *faecalis* in pulpal infections has been elucidated, there are several limitations to this  
318 study. The methods employed to fluorescently localise the bacteria could potentially  
319 result in diffusion-related artefacts. More specific post-processing techniques, such  
320 as fluorescent in-situ hybridization (FISH) probes may allow for more specific  
321 identification, quantification and localisation of mixed species pulpal infections.

322 Whilst the *ex vivo* model offers a 3D organotypic culture setting, the static nature,  
323 which lacks blood flow does not allow full observation of the systemic immune  
324 response. Potential methods to overcome this may involve addition of monocytes  
325 directly to the culture media and prolonged incubation times to stimulate repair  
326 mechanisms. Closer examination of attachment mechanisms using ACE negative *E.*  
327 *faecalis* mutants and purified LTA would also help fully establish the pathogenicity of  
328 *E. faecalis* in pulpal infections. This will allow the model to be used to develop more  
329 effective treatments for pulpitis by assessing the efficacy of antimicrobial and anti-  
330 inflammatory treatments to inhibit bacterial colonisation.

331 In conclusion, this study has modelled a mixed species pulpal infection consisting  
332 of *S. anginosus* and *E. faecalis* using a validated *ex vivo* rat tooth model. Although *E.*  
333 *faecalis* caused *S. anginosus* to reach log growth phase more rapidly, the mixed  
334 species infection did not result in higher cell death, attachment or inflammatory  
335 response from the dental pulp. *E. faecalis* was found to elicit a much greater  
336 inflammatory response, which was due to higher levels of attachment to the dental  
337 pulp, with a particular affinity to the pulpal vasculature. Future work will focus on  
338 assessing the mechanisms and attachment kinetics in order to elucidate the  
339 molecular process and rate at which *E. faecalis* colonises the pulp.

340

## 341 **Materials and Methods**

### 342 *Materials*

343 All reagents including culture media, broths and agars were purchased from  
344 Thermo Scientific (Leicestershire, UK) unless otherwise stated.

345

### 346 *Bacterial identification*

347 The *S. anginosus* and *E. faecalis* species studied were clinical isolates selected  
348 from the culture collection of the Oral Microbiology Unit, School of Dentistry at Cardiff  
349 University. To confirm the identity of the species, standard microbial identification  
350 tests were performed by assessing: colony appearance on blood agar, Gram  
351 staining, haemolysis, presence of catalase, lactose fermentation (MacConkey agar),  
352 Lancefield grouping and bile aesculin agar growth.

353 16S rRNA sequencing was also performed on the *S. anginosus* and *E. faecalis*  
354 clinical isolates to validate species identity. *S. anginosus* and *E. faecalis* were  
355 cultured overnight in brain heart infusion (BHI) broth at 37°C, 5% CO<sub>2</sub>. DNA was  
356 extracted from using a QIAamp DNA Mini Kit (Qiagen, Manchester, UK), according  
357 to the manufacturer's instructions. DNA was used in a PCR reaction using 16S  
358 rRNA bacterial universal primers D88 (F primer; 5'-GAGAGTTTGATYMTGGCTCAG-  
359 3') and E94 (R primer; 5'-GAAGGAGGTGWTCARCCGCA-3') (42) and sequencing  
360 of the products was performed by Central Biotechnology Services (Cardiff University)  
361 using a 3130xl Genetic Analyser (Applied Biosystems). DNA sequences were  
362 aligned with GenBank sequences using BLAST (NCBI) to establish percentage  
363 sequence identity.

364

#### 365 *Growth curves*

366 Overnight cultures of *S. anginosus* and *E. faecalis* in BHI broth were prepared  
367 and diluted to 10<sup>8</sup> colony forming units/mL (CFU/mL, absorbance at 600nm=0.08-  
368 0.1). The inoculum was diluted in BHI to give a starting concentration of 10<sup>2</sup>  
369 CFU/mL. Mixed species planktonic cultures with a total of 10<sup>2</sup> CFU/mL were  
370 prepared consisting of 50% *S. anginosus* and 50% *E. faecalis* (herein referred to as  
371 50:50) and 90% *S. anginosus* and 10% *E. faecalis* (herein referred to as 90:10). The



372 broths were incubated at 37°C, 5% CO<sub>2</sub> and 1mL aliquots removed every 4 hours for  
373 24 hours. The absorbance of the aliquots was measured at 600nm using an Implen  
374 OD600 DiluPhotometer (München, Germany) and 50µL spiral plated on tryptic soya  
375 agar using a Don Whitley Automated Spiral Plater (West Yorkshire, UK). The  
376 remaining aliquot was then heat treated at 60°C for 30 minutes prior to spiral plating  
377 on bile aesculin agar containing 6.5%w/w sodium chloride. Heat treatment and the  
378 presence of high concentrations of bile and sodium chloride would only permit the  
379 growth of *E. faecalis* but not *S. anginosus* (43). Plates were incubated at 37°C, 5%  
380 CO<sub>2</sub> for 24 hours prior to counting. *E. faecalis* counts were subtracted from total  
381 counts to give the number of *S. anginosus* bacteria. Specific growth rate was  
382 calculated using the log phase of each growth curve and Equation 1, where  $\mu$  is the  
383 growth rate in CFU/mL per hour,  $x$  is the CFU/mL at the end of the log phase,  $x_0$  is  
384 the CFU/mL at the start of the log phase and  $t$  is the duration of the log phase in  
385 hours.

$$\mu = \frac{\ln(x-x_0)}{t} \quad [1]$$

387

### 388 *Co-culture model*

389 The co-culture rat tooth infection model was prepared as described by  
390 Roberts et al. (7). 28-day-old male Wistar rats were sacrificed under schedule 1 of  
391 the UK Animals Scientific Procedures Act, 1986 by a qualified technician at the Joint  
392 Biological Services Unit, Cardiff University for harvesting of tissue. Upper and lower  
393 incisors were extracted and the incisors were cut into 2mm thick transverse sections  
394 using a diamond-edged rotary bone saw (TAAB, Berkshire, UK). The sections were  
395 transferred to fresh sterile Dulbecco's Modified Eagle Medium (DMEM) for no more  
396 than 20 minutes before being cultured in 2mL DMEM, supplemented with 10%v/v

397 heat-inactivated fetal calf serum, 0.15mg/mL vitamin C, 200mmol/L L-glutamine,  
398 100U/mL penicillin, 100µg/mL streptomycin sulphate and 250ng/mL amphotericin B  
399 at 37°C, 5% CO<sub>2</sub> for 24 hours. Tooth slices were then washed in 2mL of phosphate  
400 buffered saline (PBS), transferred to supplemented DMEM without antibiotics and  
401 incubated overnight to remove traces of antibiotic. *S. anginosus* 39/2/14A and *E.*  
402 *faecalis* were cultured to the log phase in BHI for 8-12 hours before dilution to 10<sup>2</sup>  
403 CFU/mL in BHI. The bacteria were then used alone or combined for mixed species  
404 infections (*S. anginosus* to *E. faecalis* ratios of 50:50 and 90:10 respectively). Forty  
405 µL of 1%w/v fluorescein diacetate (FDA) in acetone was added to 2mL of the  
406 bacterial suspension and incubated for 30 minutes at 37°C, 5% CO<sub>2</sub> before being  
407 passed through a 0.22µm syringe-driven filter unit (Millipore, Oxford, UK). Bacteria  
408 captured on the filter were then resuspended in 2mL sterile supplemented DMEM  
409 without antibiotics and with 10%v/v BHI (herein referred to as DMEM-BHI) and used  
410 to inoculate one tooth slice. Tooth slices were incubated with the bacteria at 37°C, 5%  
411 CO<sub>2</sub> for 24 hours under constant agitation at 60rpm in the dark. Sterile DMEM-BHI  
412 was used as a control. After incubation the tooth slices were processed for histology  
413 in the dark. Tooth slices were fixed in 10%w/v neutral-buffered formalin at room  
414 temperature for 24 hours. Slices were demineralized in 10%w/v formic acid at room  
415 temperature for 72 hours; dehydrated through a series of 50%v/v, 70%v/v, 95%v/v,  
416 and 100%v/v ethanol followed by 100%v/v xylene for five minutes each; and  
417 embedded in paraffin wax. Sections 5µm thick were cut and viewed under a  
418 fluorescent microscope with a FITC filter, with images captured using a Nikon digital  
419 camera and ACT-1 imaging software (Nikon UK Ltd, Surrey, UK). To quantify cell  
420 viability and structural degradation, sections were stained with hematoxylin and  
421 eosin (H&E) prior to capturing images with a light microscope.

422

423 *Gram stain of tissue sections*

424 Gram stains of tooth slices were performed using a modified Brown and Brenn  
425 method (44). Paraffin-embedded tooth slices were cut using a microtome into 5µm  
426 sections and rehydrated through a series of xylene, 100, 95 and 70%v/v ethanol for  
427 five minutes each. Sections were immersed in 0.2%w/v crystal violet for 1 minute,  
428 rinsed with distilled water, immersed in Gram's iodine for 1 minute, rinsed with  
429 distilled water, decolourised with acetone for 5 seconds and counterstained for 1  
430 minute with basic fuchsin solution prior to washing with distilled water and mounting.  
431 Light microscopy images were captured at x100 magnification using a Nikon digital  
432 camera and ACT-1 imaging software (Nikon UK Ltd, Surrey, UK).

433

434 *Semi-quantification of cell viability by cell counts*

435 ImageJ (National Institutes of Health, Maryland USA) was used to count the  
436 number of nuclei per pulp on stained histological sections. For each time point,  
437 sections were cut from 5 tooth slices. Images were captured at x20 magnification  
438 and combined using ImageJ software (Fig. S6). The blue field was extracted from  
439 the images and the moments threshold method was applied to separate the pulp  
440 cells. The watershed function was applied to split adjacent cell nuclei and the  
441 number of particles ranging in size from 3 to 100µm<sup>2</sup> were counted. The data was  
442 normalised to the pulpal area and standard errors of the mean were calculated.

443

444 *Semi-quantification of bacterial coverage*

445 ImageJ was used to quantify the area of the pulp inoculated with fluorescent  
446 bacteria. The green field of the fluorescent image was extracted and the image

447 converted into a binary form using the moments threshold method. The pulpal area  
448 was manually selected and the total area of the pulp measured. The area covered  
449 by the fluorescent bacteria was then measured and calculated as a percentage of  
450 the selected pulp area (Fig. S7).

451

#### 452 *RT-qPCR of cytokines*

453 Four mm thick tooth slices were cultured as previously described for 24 hours  
454 with either sterile DMEM-BHI as a control; DMEM-BHI inoculated with  $10^2$ CFU/mL  
455 *S.anginosus* or *E. faecalis* or DMEM-BHI with a mixed species of *S.anginosus* or *E.*  
456 *faecalis* (50:50 and 90:10 ratios respectively). After incubation, the tooth slice was  
457 transferred to sterile PBS and the pulp removed by flushing the pulpal cavity with  
458 PBS using a 0.1mm needle and syringe. RNA was extracted using TRIzol® Reagent  
459 (ThermoFisher Scientific, Loughborough, UK) followed by RNase treatment  
460 (Promega, Southampton, UK) according to the manufacturers' instructions.

461 Analysis of gene expression was performed in accordance to the Minimum  
462 Information for publication of Quantitative real-time PCR Experiments (MIQE)  
463 guidelines (45). RNA concentrations were determined using a NanoVue  
464 Spectrophotometer (GE Healthcare Life Sciences, Buckinghamshire, UK). RNA  
465 purity was determined by ensuring the ratio of absorbance at 260/280nm was above  
466 1.8 and RNA quality checked by separating 1µg of RNA electrophoretically on a 2%  
467 agarose gel containing SafeView (NBS Biologicals, Cambridgeshire, UK) in  
468 Tris/Borate/EDTA buffer to ensure intact 28S and 18S rRNA bands using a Gel  
469 Doc™ EZ System (BioRad, Hertfordshire, UK). Fig. S8 demonstrates RNA integrity  
470 following extraction for samples tested.

471 Complementary DNA (cDNA) was synthesized by reverse transcription using  
472 Promega reagents (Southampton, UK) in a G-Storm GS1 thermocycler (Somerton,  
473 UK). One µg extracted RNA was combined with 1µL random primer in a 15µL  
474 reaction in nuclease free water at 70°C for 5 minutes. This suspension was added to  
475 5µL MMLV reaction buffer, 1.25µL deoxyribonucleotide triphosphates (10mM stock  
476 dNTPSs), 0.6µL RNasin, 1µL MMLV enzyme and 2.15µL nuclease free water and  
477 incubated at 37°C for 1 hour.

478 The resultant cDNA was diluted 1:10 in nuclease free water (25ng cDNA).  
479 Forward and reverse primers used are listed in Table 2. Ten µL of PrecisionFAST  
480 qPCR SYBR Green MasterMix with low ROX (Primerdesign, Chandler's Ford, United  
481 Kingdom) was combined with 2µL of forward and 2µL of reverse primers (3µM) with  
482 1µL nuclease-free water prior to addition of 5µL cDNA in BrightWhite Real-time PCR  
483 FAST 96-well plates (Primerdesign, Chandler's Ford, United Kingdom). The plates  
484 were subsequently heated to 95°C for 20 seconds; then 40 cycles of: 95°C for 1  
485 second and 55°C for 20 seconds; followed by melt-curve analysis at 95°C for 15  
486 seconds, 60°C for 60 seconds and 95°C for 15 seconds in a QuantStudio™ 6 Flex  
487 Real-Time PCR System with QuantStudio Real-Time PCR Software (ThermoFisher  
488 Scientific, Loughborough, UK). Relative TNF-α and IL-1β gene expression was  
489 calculated with beta actin (β-actin) as the reference gene and uninfected samples as  
490 the control using the Livak method (46).

491 Primer specificity was ensured by the presence of single melt curve peaks (Fig.  
492 S9) and by running products on agarose gels, as previously described, to confirm  
493 single bands and correct product lengths (Fig. S10). Primer efficiency was between  
494 90-110% for all primers used (Fig. S11) and determined using total rat RNA  
495 converted to cDNA, as previously described, and serially diluted 1:4 in nuclease-free

496 water. Reference gene validation was performed by comparing gene stability across  
497 all samples using NormFinder software (47).  $\beta$ -actin was found to be the most stable  
498 reference gene (Fig. S12).

499

#### 500 *TNF- $\alpha$ and IL-1 $\beta$ Immunohistochemistry*

501 Immunohistochemical staining of the tooth slices for TNF- $\alpha$  and IL-1 $\beta$  was  
502 performed based on methods used by Smith et al (48). Rat lung was used as a  
503 positive control for TNF- $\alpha$  and IL-1 $\beta$  following fixation in 10%w/v neutral-buffered  
504 formalin at room temperature for 24 hours, dehydration through a series of 50%v/v,  
505 70%v/v, 95%v/v, and 100%v/v ethanol followed by 100%v/v xylene for five minutes  
506 each; and embedding in paraffin wax. Paraffin-embedded tooth slices and lung  
507 samples were cut using a microtome into 5  $\mu$ m sections and incubated on glass  
508 slides at 65°C for one hour. The samples were subsequently rehydrated through a  
509 series of xylene, 100%v/v, 95%v/v and 70%v/v ethanol and double-distilled water for  
510 5 minutes each. Endogenous peroxidase activity within the tissue sections was  
511 quenched by incubation in 3%w/v hydrogen peroxide for 10 minutes, followed by 2  
512 washes for 2 minutes in tris-buffered saline (TBS). Non-specific binding was blocked  
513 with 3%v/v normal horse serum (Vector laboratories, Peterborough, UK) in TBS for  
514 30 minutes. Sections were incubated for 1 hour with primary antibodies for TNF- $\alpha$   
515 and IL-1 $\beta$  (Santa Cruz Biotechnology, Heidelberg, Germany) diluted 1:50 in TBS  
516 containing 1%w/v bovine serum albumin (Sigma Aldrich, Gillingham, UK).  
517 Immunoreactivity was then performed using a Vectastain ABC peroxidase detection  
518 kit (Vector laboratories, Peterborough, UK). Negative controls included omission of  
519 the primary antibody and replacements of the primary antibody with immunoglobulin  
520 G isotype diluted to the working concentration of the primary antibody. Sections

521 were counterstained with 0.05% light green for 30 seconds, dehydrated with 100%  
522 ethanol and xylene for 10 minutes each and mounted using VectaMount Permanent  
523 Mounting Medium (Vector laboratories, Peterborough, UK) prior to imaging using a  
524 Nikon digital camera and ACT-1 imaging software (Nikon UK Ltd, Surrey, UK).

525

#### 526 *SDS-PAGE of bacterial proteins*

527 An overnight culture of *S. anginosus* and *E. faecalis* in BHI was prepared and  
528 diluted to  $10^2$  CFU/mL. *S. anginosus* and *E. faecalis* were cultured at 37°C, 5% CO<sub>2</sub>  
529 for 24 hours alone or in combination at a ratio of 50:50 and 90:10 respectively. The  
530 suspensions were centrifuged at 5000g for 5 minutes. The supernatant was used for  
531 analysis of supernatant proteins. The pellet was lysed in RIPA buffer by vortexing  
532 for 30 seconds followed by 30 seconds ultrasonication at 50 Joules using a Branson  
533 SLPe sonifier (Connecticut, USA). Protein concentrations in the supernatant and the  
534 bacterial pellet were quantified using a BCA assay (ThermoFisher Scientific,  
535 Loughborough, UK) and 20µg of protein in Laemmli buffer (Biorad, Hertfordshire, UK)  
536 separated by SDS-PAGE at 200V for 40 minutes. Gels were stained using a Biorad  
537 Silver Stain Plus Kit according to the manufacturer's instructions and imaged using a  
538 Gel Doc™ EZ System (Biorad, Hertfordshire, UK).

539

#### 540 *E. faecalis* supernatant and heat-killed *E. faecalis* treatments

541 An overnight culture of *E. faecalis* was diluted in 20mL DMEM-BHI media to give  
542 a starting inoculum of  $10^2$ CFU/mL as previously described. After incubation for an  
543 additional 24 hours at 37°C, 5% CO<sub>2</sub>, the suspension was centrifuged at 5000g for 5  
544 minutes. The supernatant was filtered through a 0.22µm syringe filter and frozen  
545 overnight at -20°C before freeze drying for 24 hours using a ScanVac CoolSafe

546 freeze dryer (LaboGene, Lyngø, Denmark). The pellet of bacteria was resuspended  
547 in 20mL of PBS and centrifuged at 5000g for 5 minutes. This step was repeated  
548 again to ensure minimal carryover of culture supernatant. The pellet was then  
549 resuspended in 20mL DMEM-BHI and heated to 100°C for one hour. The solution  
550 was then frozen overnight at -20°C before freeze drying as previously described.  
551 20mL of sterile DMEM-BHI was also frozen and freeze dried as a control. All freeze  
552 dried samples were individually resuspended in 20mL of sterile DMEM-BHI and used  
553 to culture rat tooth slices for RT-qPCR of cytokines and immunohistochemistry of  
554 TNF- $\alpha$  and IL-1 $\beta$  as previously described.

555

#### 556 *Statistical analysis*

557 A one-way analysis of variance (ANOVA) was performed using the data analysis  
558 package in Excel (Microsoft, Reading, UK) to determine the relative significance of  
559 the difference between the infected groups and the controls in terms of cell counts,  
560 bacterial coverage and cytokine expression. The Tukey-Kramer test was used in  
561 conjunction with ANOVA to compare the significant difference between all possible  
562 pairs of means.  $P \leq 0.05$  was considered significant.

563

#### 564 **Acknowledgements**

565 This work was supported by The Dunhill Medical Trust [grant number:  
566 R232/1111].

567

#### 568 **References**

- 569 1. Nanci A. 2013. Dentin-pulp complex, p 183, Ten cate's oral histology:  
570 Development, structure, and function, 8th ed. Mosby Elsevier, St. Louis, MO.



- 571 2. Ng YL, Mann V, Rahbaran S, Lewsey J, Gulabivala K. 2007. Outcome of  
572 primary root canal treatment: Systematic review of the literature - Part 1.  
573 Effects of study characteristics on probability of success. *Int Endod J* 40:921-  
574 39.
- 575 3. Mukhaimer R, Hussein E, Orafi I. 2012. Prevalence of apical periodontitis and  
576 quality of root canal treatment in an adult palestinian sub-population. *The*  
577 *Saudi Dental Journal* 24:149-155.
- 578 4. Berlinck T, Tinoco JMM, Carvalho FLF, Sassone LM, Tinoco EMB. 2015.  
579 Epidemiological evaluation of apical periodontitis prevalence in an urban  
580 brazilian population. *Brazilian Oral Research* 29:1-7.
- 581 5. AAPD. 2016. Guideline on pulp therapy for primary and immature permanent  
582 teeth. *Pediatr Dent* 38:280-288.
- 583 6. Demarco FF, Rosa MS, Tarquínio SBC, Piva E. 2005. Influence of the  
584 restoration quality on the success of pulpotomy treatment: A preliminary  
585 retrospective study. *Journal of Applied Oral Science* 13:72-77.
- 586 7. Roberts JL, Maillard JY, Waddington RJ, Denyer SP, Lynch CD, Sloan AJ.  
587 2013. Development of an *ex vivo* coculture system to model pulpal infection  
588 by *Streptococcus anginosus* group bacteria. *J Endod* 39:49-56.
- 589 8. Jenkinson HF, Demuth DR. 1997. Structure, function and immunogenicity of  
590 streptococcal antigen I/II polypeptides. *Mol Microbiol* 23:183-90.
- 591 9. Shweta S, Prakash SK. 2013. Dental abscess: A microbiological review.  
592 *Dental Research Journal* 10:585-591.

- 593 10. Bik EM, Long CD, Armitage GC, Loomer P, Emerson J, Mongodin EF, Nelson  
594 KE, Gill SR, Fraser-Liggett CM, Relman DA. 2010. Bacterial diversity in the  
595 oral cavity of ten healthy individuals. *The ISME journal* 4:962-974.
- 596 11. Rôças IN, Alves FRF, Rachid CT, Lima KC, Assunção IV, Gomes PN,  
597 Siqueira JF, Jr. 2016. Microbiome of deep dentinal caries lesions in teeth with  
598 symptomatic irreversible pulpitis. *PLOS ONE* 11:e0154653.
- 599 12. Hahn CL, Liewehr FR. 2007. Relationships between caries bacteria, host  
600 responses, and clinical signs and symptoms of pulpitis. *Journal of*  
601 *Endodontics* 33:213-219.
- 602 13. Suchitra U, Kundabala M. 2006. *Enterococcus faecalis*: An endodontic  
603 pathogen. *Endodontology* 18:11-13.
- 604 14. Sundqvist G, Figdor D, Persson S, Sjogren U. 1998. Microbiologic analysis of  
605 teeth with failed endodontic treatment and the outcome of conservative re-  
606 treatment. *Oral Surg Oral Med Oral Pathol Oral Radiol Endod* 85:86-93.
- 607 15. Stuart CH, Schwartz SA, Beeson TJ, Owatz CB. 2006. *Enterococcus faecalis*:  
608 Its role in root canal treatment failure and current concepts in retreatment. *J*  
609 *Endod* 32:93-8.
- 610 16. Salah R, Dar-Odeh N, Abu Hammad O, Shehabi AA. 2008. Prevalence of  
611 putative virulence factors and antimicrobial susceptibility of *Enterococcus*  
612 *faecalis* isolates from patients with dental diseases. *BMC Oral Health* 8:17.

- 613 17. Hegde A, Lakshmi P. 2013. Prevalence of selected microorganisms in the  
614 pulp space of human deciduous teeth with irreversible pulpitis. *Endodontolgy*  
615 25:107-111.
- 616 18. Brown SA, Whiteley M. 2007. A novel exclusion mechanism for carbon  
617 resource partitioning in *Aggregatibacter actinomycetemcomitans*. *Journal of*  
618 *Bacteriology* 189:6407-6414.
- 619 19. Ramsey MM, Whiteley M. 2009. Polymicrobial interactions stimulate  
620 resistance to host innate immunity through metabolite perception.  
621 *Proceedings of the National Academy of Sciences* 106:1578-1583.
- 622 20. Ramsey MM, Rumbaugh KP, Whiteley M. 2011. Metabolite cross-feeding  
623 enhances virulence in a model polymicrobial infection. *PLOS Pathogens*  
624 7:e1002012.
- 625 21. Fabricius L, Dahlen G, Sundqvist G, Happonen RP, Moller AJ. 2006.  
626 Influence of residual bacteria on periapical tissue healing after  
627 chemomechanical treatment and root filling of experimentally infected monkey  
628 teeth. *Eur J Oral Sci* 114:278-85.
- 629 22. Cook LC, LaSarre B, Federle MJ. 2013. Interspecies communication among  
630 commensal and pathogenic streptococci. *mBio* 4.
- 631 23. Lancefield RC. 1933. A serological differentiation of human and other groups  
632 of hemolytic streptococci. *The Journal of Experimental Medicine* 57:571-595.

- 633 24. Guzmàn CA, Pruzzo C, Platé M, Guardati MC, Calegari L. 1991. Serum  
634 dependent expression of *Enterococcus faecalis* adhesins involved in the  
635 colonization of heart cells. *Microbial Pathogenesis* 11:399-409.
- 636 25. Fisher K, Phillips C. 2009. The ecology, epidemiology and virulence of  
637 enterococcus. *Microbiology* 155:1749-57.
- 638 26. Nallapareddy SR, Qin X, Weinstock GM, Höök M, Murray BE. 2000.  
639 *Enterococcus faecalis* adhesin, ace, mediates attachment to extracellular  
640 matrix proteins collagen type iv and laminin as well as collagen type i.  
641 *Infection and Immunity* 68:5218-5224.
- 642 27. Singh KV, Nallapareddy SR, Sillanpaa J, Murray BE. 2010. Importance of the  
643 collagen adhesin ace in pathogenesis and protection against *Enterococcus*  
644 *faecalis* experimental endocarditis. *PLoS Pathogens* 6:e1000716.
- 645 28. Allen BL, Katz B, Hook M. 2002. *Streptococcus anginosus* adheres to  
646 vascular endothelium basement membrane and purified extracellular matrix  
647 proteins. *Microbial Pathogenesis* 32:191-204.
- 648 29. Gong Q, He L, Liu Y, Zhong J, Wang S, Xie M, Sun S, Zheng J, Xiang L,  
649 Ricupero CL, Nie H, Ling J, Mao JJ. 2017. Biomaterials selection for dental  
650 pulp regeneration, p 159-173. *In* Ducheyne P (ed), *Comprehensive*  
651 *biomaterials II*, 2nd ed. Elsevier, Oxford.
- 652 30. Guzmàn CA, Pruzzo C, Li Pira G, Calegari L. 1989. Role of adherence in  
653 pathogenesis of *Enterococcus faecalis* urinary tract infection and endocarditis.  
654 *Infection and Immunity* 57:1834-1838.

- 655 31. Park OJ, Han JY, Baik JE, Jeon JH, Kang SS, Yun CH, Oh JW, Seo HS, Han  
656 SH. 2013. Lipoteichoic acid of *Enterococcus faecalis* induces the expression  
657 of chemokines via tlr2 and pafr signaling pathways. J Leukoc Biol 94:1275-84.
- 658 32. de Oliveira LA, Barbosa SV. 2003. The reaction of dental pulp to *Escherichia*  
659 *coli* lipopolysaccharide and *Enterococcus faecalis* lipoteichoic acid. Brazilian  
660 Journal of Microbiology 34:179-181.
- 661 33. Baik JE, Ryu YH, Han JY, Im J, Kum KY, Yun CH, Lee K, Han SH. 2008.  
662 Lipoteichoic acid partially contributes to the inflammatory responses to  
663 *Enterococcus faecalis*. J Endod 34:975-82.
- 664 34. Wang S, Liu KUN, Seneviratne CJ, Li X, Cheung GSP, Jin L, Chu CH, Zhang  
665 C. 2015. Lipoteichoic acid from an *Enterococcus faecalis* clinical strain  
666 promotes tnf- $\alpha$  expression through the nf-kb and p38 mapk signaling  
667 pathways in differentiated thp-1 macrophages. Biomedical Reports 3:697-702.
- 668 35. Jontell M, Gunraj MN, Bergenholtz G. 1987. Immunocompetent cells in the  
669 normal dental pulp. J Dent Res 66:1149-53.
- 670 36. Okiji T, Jontell M, Belichenko P, Dahlgren U, Bergenholtz G, Dahlstrom A.  
671 1997. Structural and functional association between substance p- and  
672 calcitonin gene-related peptide-immunoreactive nerves and accessory cells in  
673 the rat dental pulp. J Dent Res 76:1818-24.
- 674 37. Jontell M, Okiji T, Dahlgren U, Bergenholtz G. 1998. Immune defense  
675 mechanisms of the dental pulp. Crit Rev Oral Biol Med 9:179-200.

- 676 38. Chivatxaranukul P, Dashper SG, Messer HH. 2008. Dentinal tubule invasion  
677 and adherence by *Enterococcus faecalis*. International Endodontic Journal  
678 41:873-882.
- 679 39. Veerayutthwilai O, Byers MR, Pham TT, Darveau RP, Dale BA. 2007.  
680 Differential regulation of immune responses by odontoblasts. Oral Microbiol  
681 Immunol 22:5-13.
- 682 40. Durand SH, Flacher V, Romeas A, Carrouel F, Colomb E, Vincent C, Magloire  
683 H, Couble ML, Bleicher F, Staquet MJ, Lebecque S, Farges JC. 2006.  
684 Lipoteichoic acid increases tlr and functional chemokine expression while  
685 reducing dentin formation in *in vitro* differentiated human odontoblasts. J  
686 Immunol 176:2880-7.
- 687 41. Jiang HW, Zhang W, Ren BP, Zeng JF, Ling JQ. 2006. Expression of toll like  
688 receptor 4 in normal human odontoblasts and dental pulp tissue. J Endod  
689 32:747-51.
- 690 42. Paster BJ, Boches SK, Galvin JL, Ericson RE, Lau CN, Levanos VA,  
691 Sahasrabudhe A, Dewhirst FE. 2001. Bacterial diversity in human subgingival  
692 plaque. J Bacteriol 183:3770-83.
- 693 43. Kumar S. 2012. Textbook of microbiology, p 251, 1st ed. Jaypee Brothers  
694 Medical Publishers, London, UK.
- 695 44. Bancroft JD, Gamble M. 2008. Microorganisms, p 312, Theory and practice of  
696 histological techniques, 8th ed. Churchill Livingstone, London, UK.

- 697 45. Bustin SA, Benes V, Garson JA, Hellemans J, Huggett J, Kubista M, Mueller  
698 R, Nolan T, Pfaffl MW, Shipley GL, Vandesompele J, Wittwer CT. 2009. The  
699 MIQE guidelines: Minimum information for publication of quantitative real-time  
700 pcr experiments. Clin Chem 55:611-22.
- 701 46. Livak KJ, Schmittgen TD. 2001. Analysis of relative gene expression data  
702 using real-time quantitative PCR and the  $2^{-(\Delta\Delta C_t)}$  method. Methods  
703 25:402-8.
- 704 47. Andersen CL, Jensen JL, Orntoft TF. 2004. Normalization of real-time  
705 quantitative reverse transcription-pcr data: A model-based variance estimation  
706 approach to identify genes suited for normalization, applied to bladder and  
707 colon cancer data sets. Cancer Res 64:5245-50.
- 708 48. Smith EL, Locke M, Waddington RJ, Sloan AJ. 2010. An *ex vivo* rodent  
709 mandible culture model for bone repair. Tissue Eng Part C Methods 16:1287-  
710 96.
- 711 49. Xing W, Deng M, Zhang J, Huang H, Dirsch O, Dahmen U. 2009. Quantitative  
712 evaluation and selection of reference genes in a rat model of extended liver  
713 resection. J Biomol Tech 20:109-115.
- 714 50. Harrington J, Sloan AJ, Waddington RJ. 2014. Quantification of clonal  
715 heterogeneity of mesenchymal progenitor cells in dental pulp and bone  
716 marrow. Connective Tissue Research 55:62-67.
- 717 51. Seol D, Choe H, Zheng H, Jang K, Ramakrishnan PS, Lim T-H, Martin JA.  
718 2011. Selection of reference genes for normalization of quantitative real-time  
719 PCR in organ culture of the rat and rabbit intervertebral disc. BMC Research  
720 Notes 4:1-8.

- 721 52. Langnaese K, John R, Schweizer H, Ebmeyer U, Keilhoff G. 2008. Selection  
722 of reference genes for quantitative real-time PCR in a rat asphyxial cardiac  
723 arrest model. BMC Molecular Biology 9:53-53.
- 724 53. Lardizábal MN, Nocito AL, Daniele SM, Ornella LA, Palatnik JF, Veggi LM.  
725 2012. Reference genes for real-time PCR quantification of micornas and  
726 messenger RNAs in rat models of hepatotoxicity. PLoS ONE 7:e36323.
- 727 54. Qiang L, Lin HV, Kim-Muller JY, Welch CL, Gu W, Accili D. 2011.  
728 Proatherogenic abnormalities of lipid metabolism in SirT1 transgenic mice are  
729 mediated through creb deacetylation. Cell metabolism 14:758-767.

730

### 731 **Figure legends**

732 Fig. 1: Growth curves of (A) *E. faecalis*, (B) *S. anginosus*, *E. faecalis* and *S.*  
733 *anginosus* combined at a ratio of (C) 50:50 and (D) 90:10 respectively. Mean values  
734 of three experimental repeats shown with error bars indicating standard deviation.

735

736 Fig. 2: Gram stain of tooth slices infected with (A) *E. faecalis*, (B) 50:50 *S.*  
737 *anginosus* : *E. faecalis* and (C to E) 90:10 *S. anginosus* : *E. faecalis*. Arrows  
738 highlight areas of bacterial attachment, P represents dental pulp, D represents  
739 dentine and S represents soft tissue surrounding the tooth. Representative images  
740 of three experimental repeats shown.

741

742 Fig. 3: Localisation of bacterial attachment by fluorescent microscopy for tooth slices  
743 infected with: (A) No bacteria control, (B) *E. faecalis*, (C) *S. anginosus*, (D) 50:50 *S.*  
744 *anginosus* : *E. faecalis* and (E) 90:10 *S. anginosus* : *E. faecalis*. P represents the  
745 dental pulp, O the odontoblast region and D the dentine. Representative images of



746 three experimental repeats shown. (F) Bacterial coverage as quantified by area of  
747 fluorescence relative to total pulp area (\*p≤0.05, \*\*p≤0.01 and \*\*\*p≤0.001). Mean  
748 values of three experimental repeats shown with error bars indicating standard error  
749 of the mean.

750

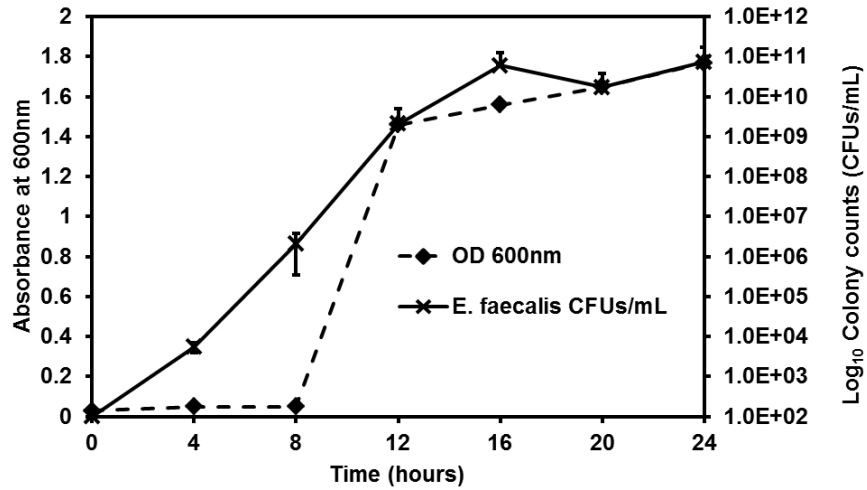
751 Fig. 4: (A) Viable cells counted per mm<sup>2</sup> of pulp. Tooth slices infected with *E.*  
752 *faecalis* and *S. anginosus*, both alone and in combination after 24 hours all resulted  
753 in a significant reduction in viable cell number in the pulp when compared to the non-  
754 infected control (\*p≤0.05). Mean values of three experimental repeats shown with  
755 error bars indicating standard error of the mean. Fold change in (B) TNF-α and (C)  
756 IL-1β gene expression as a result of *E. faecalis* and *S. anginosus* infections, alone  
757 and in combination (\*p≤0.05, \*\*p≤0.01 compared to control samples and †p≤0.05 and  
758 ††p≤0.01). Mean values of three experimental repeats shown with error bars  
759 indicating standard error of the mean. (D) Immunohistochemistry of TNF-α and IL-  
760 1β for control samples and tooth slices infected with *S. anginosus*, *E. faecalis*, 50:50  
761 *S. anginosus* : *E. faecalis* and 90:10 *S. anginosus* : *E. faecalis*, Representative  
762 images of three experimental repeats shown.

763

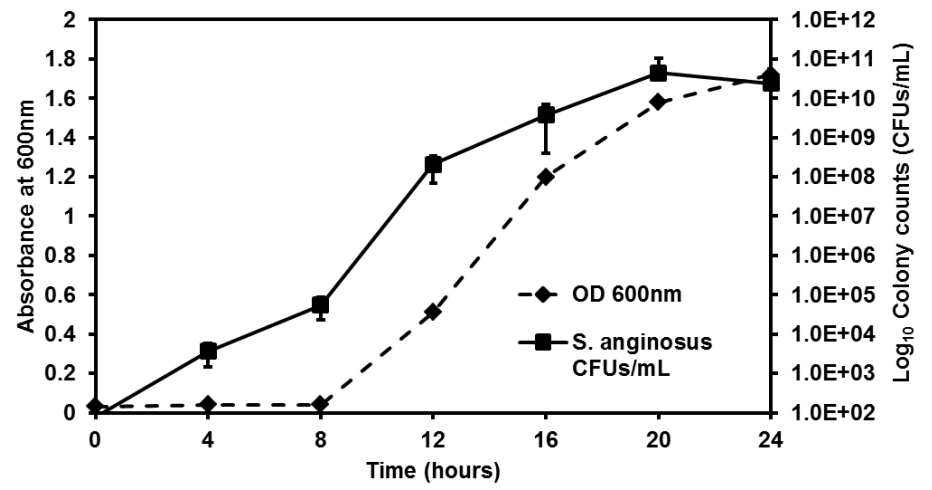
764 Fig.5: Fold change in (A) TNF-α and (B) IL-1β gene expression relative to β-actin as  
765 a result of treating tooth slices with *E. faecalis* supernatant and heat-killed *E. faecalis*  
766 (\*p≤0.05 compared to control samples). Mean values of three experimental repeats  
767 shown with error bars indicating standard error of the mean. (C)  
768 Immunohistochemistry of TNF-α and IL-1β for control samples and tooth slices  
769 infected with *E. faecalis* supernatant and heat-killed *E. faecalis*. Representative  
770 images of three experimental repeats shown.

**Fig. 1**

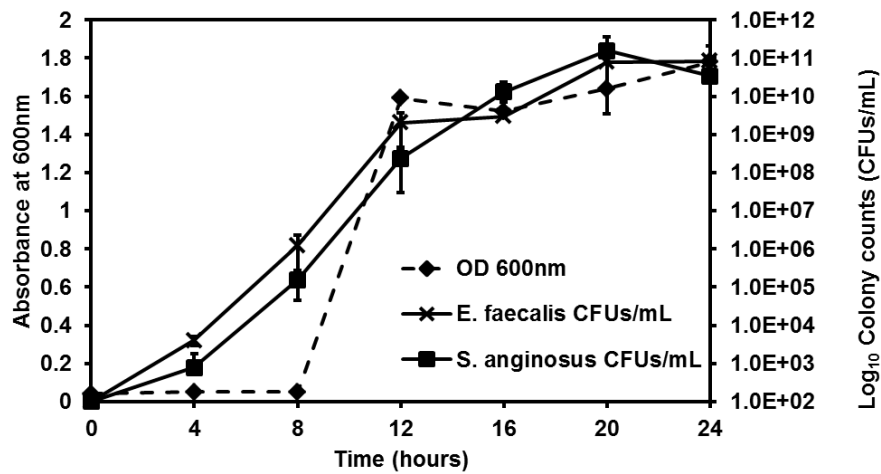
**A**



**B**



**C**



**D**

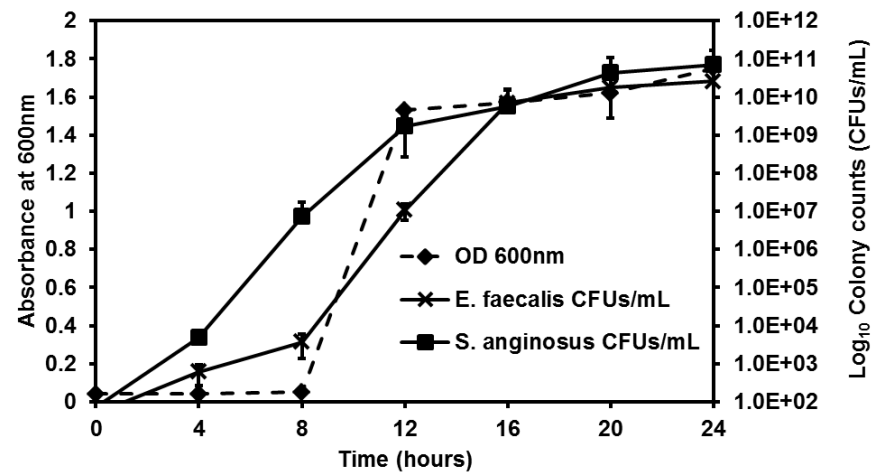


Fig. 2

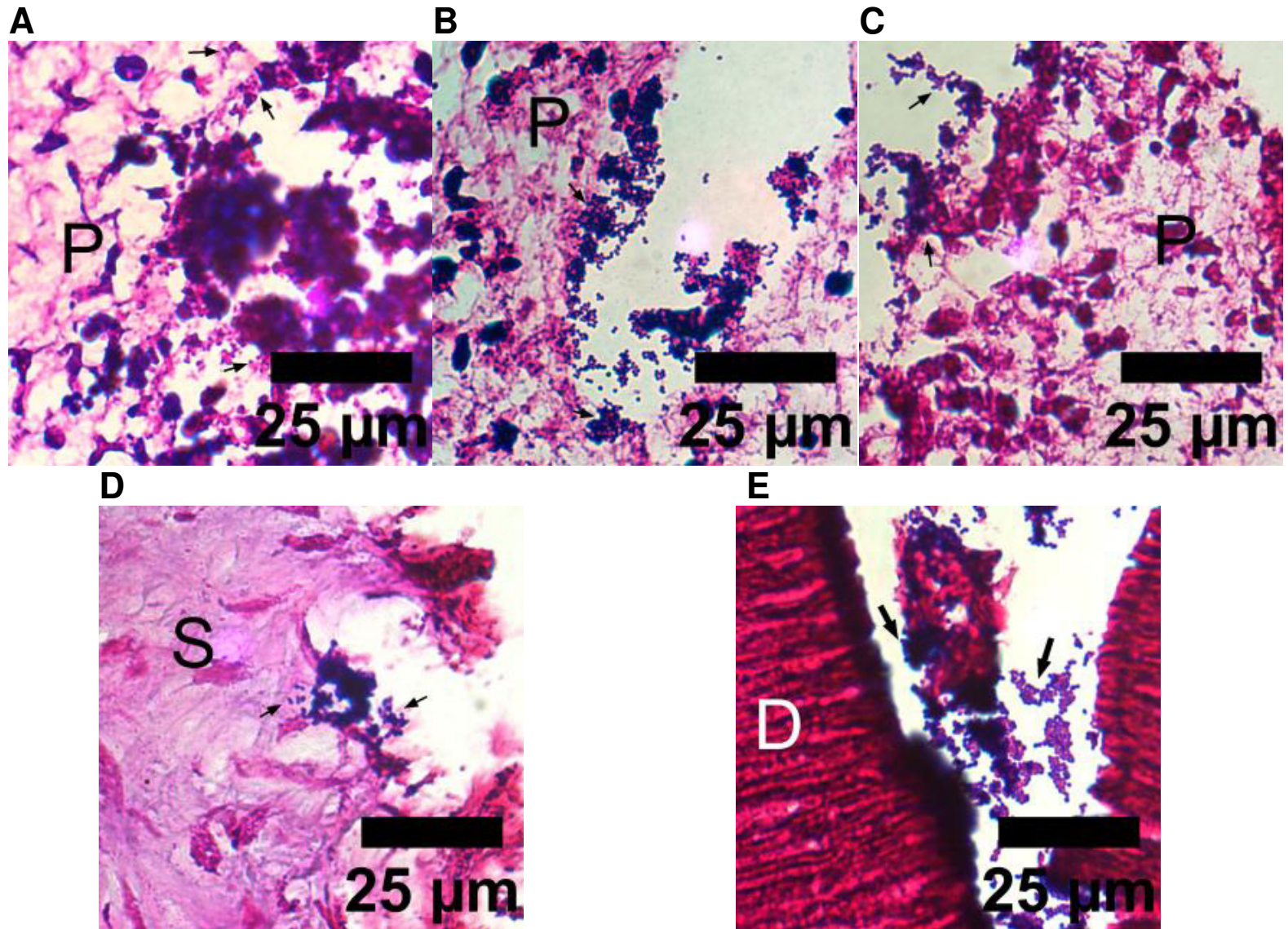
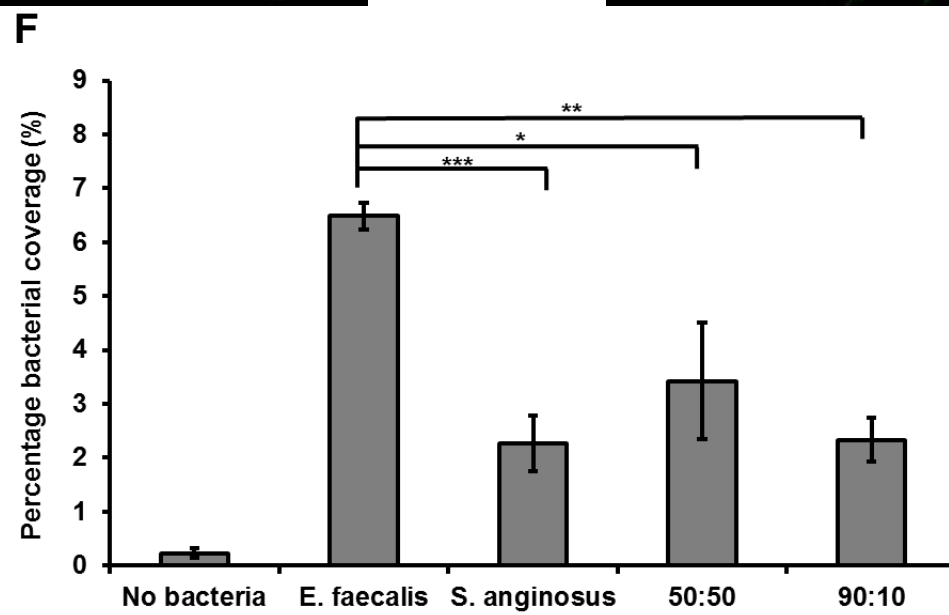
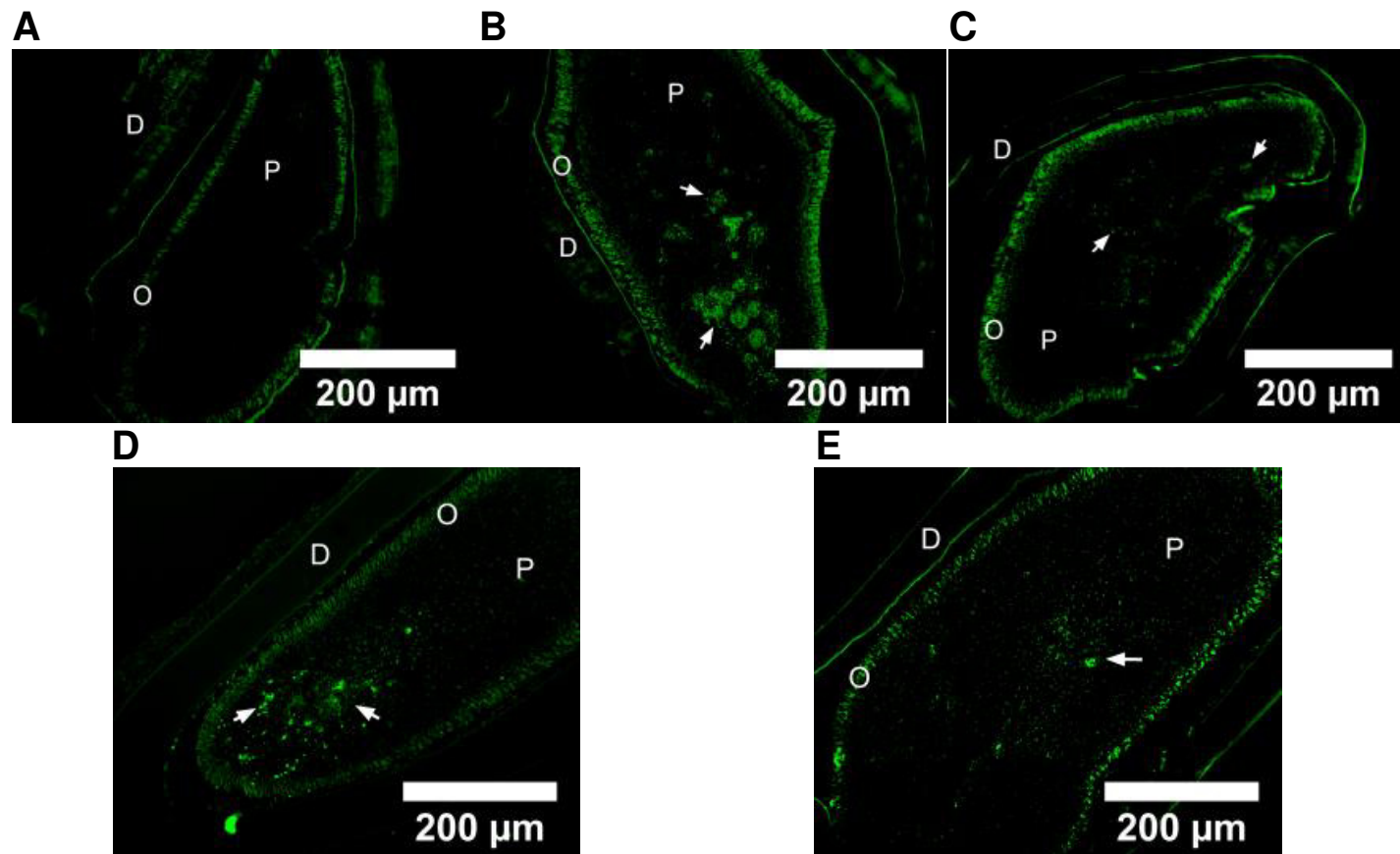
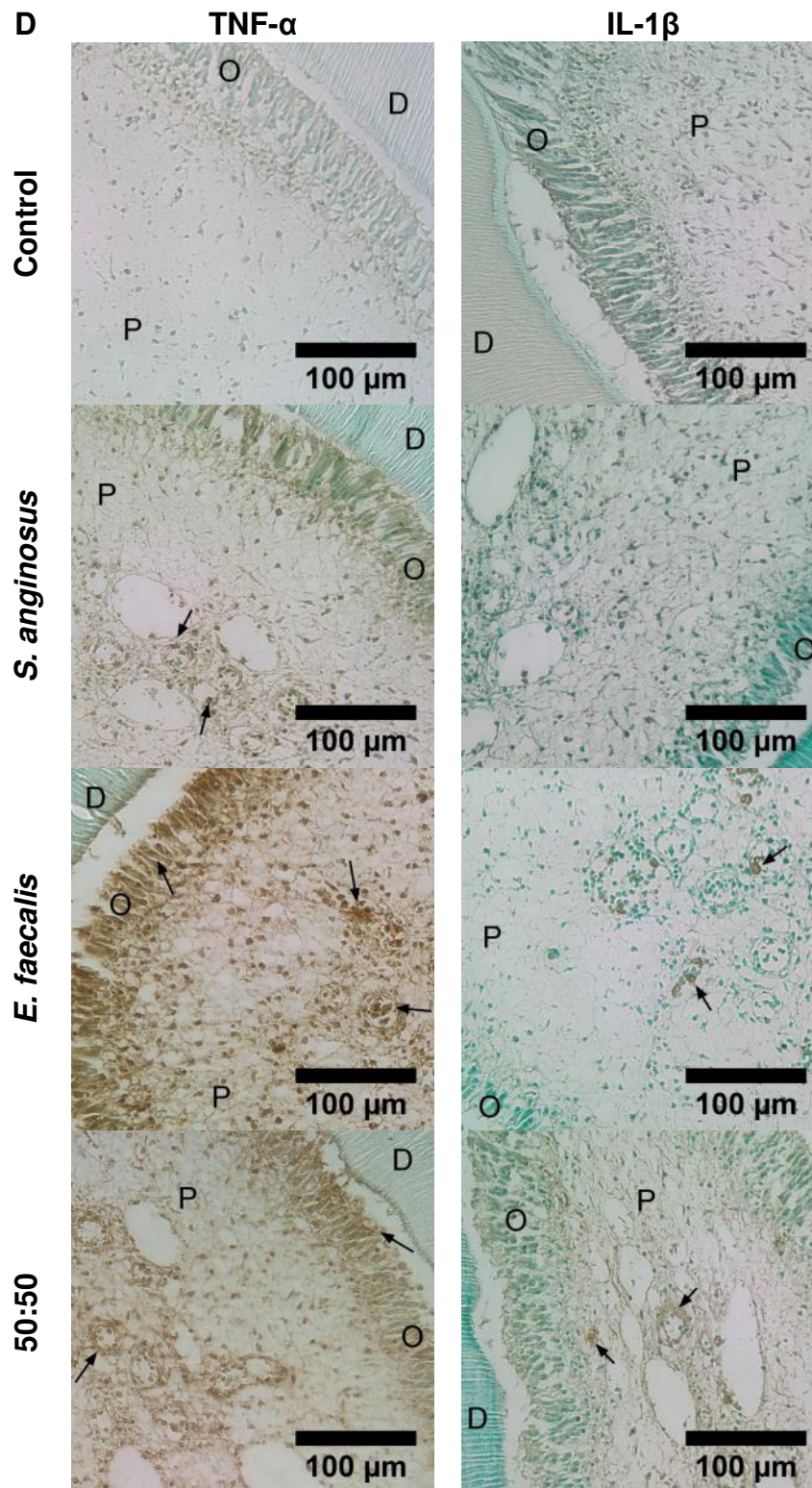
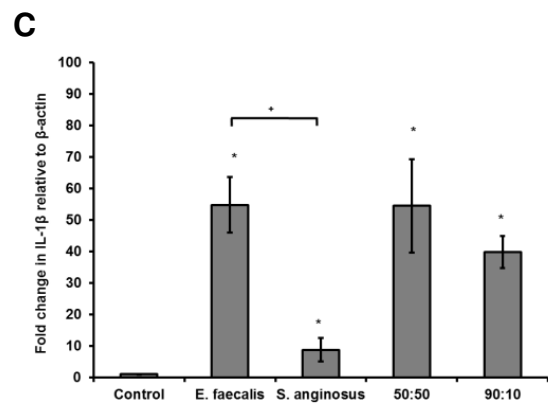
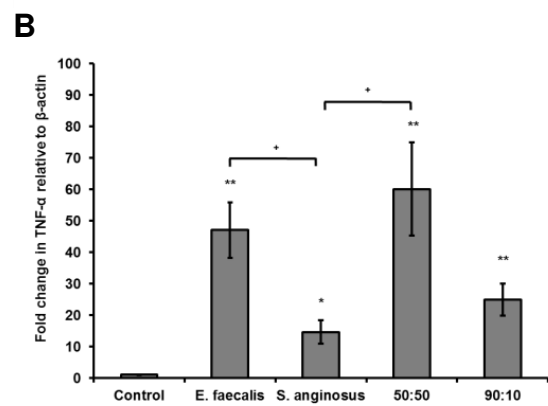
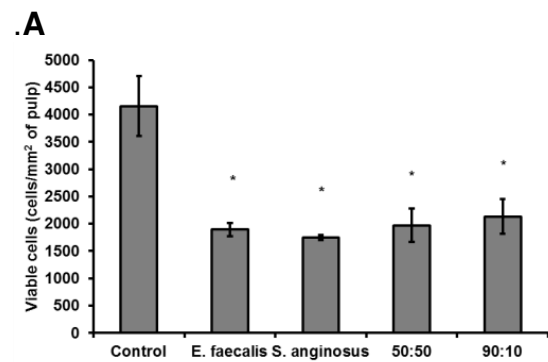


Fig. 3





**Fig. 4**





**Fig. 5**

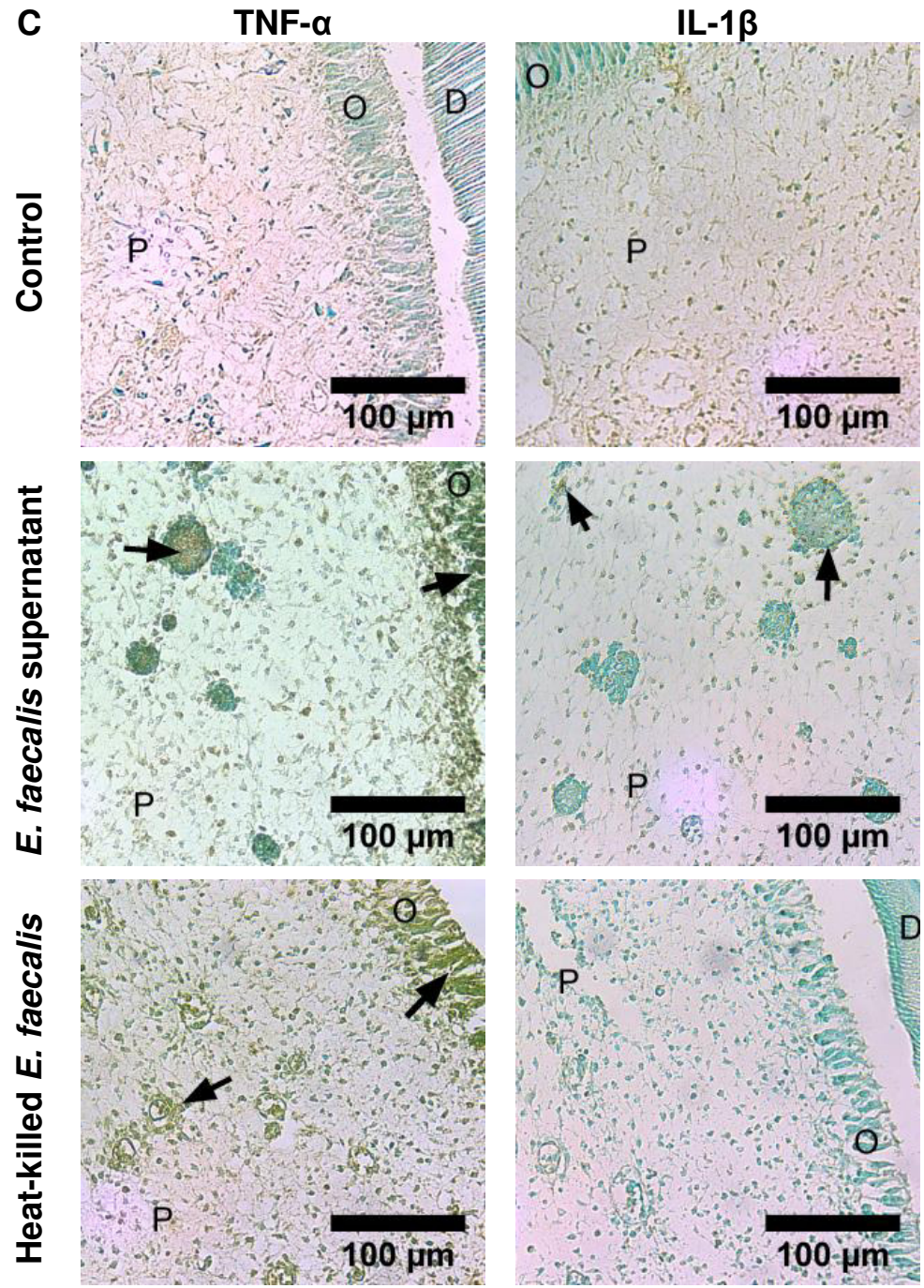
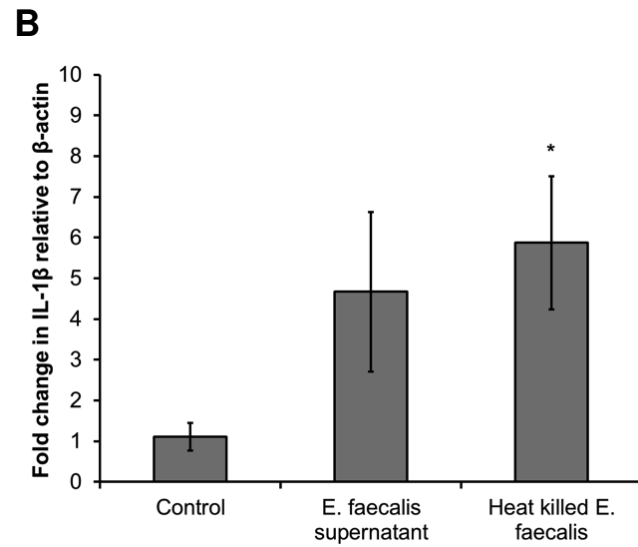
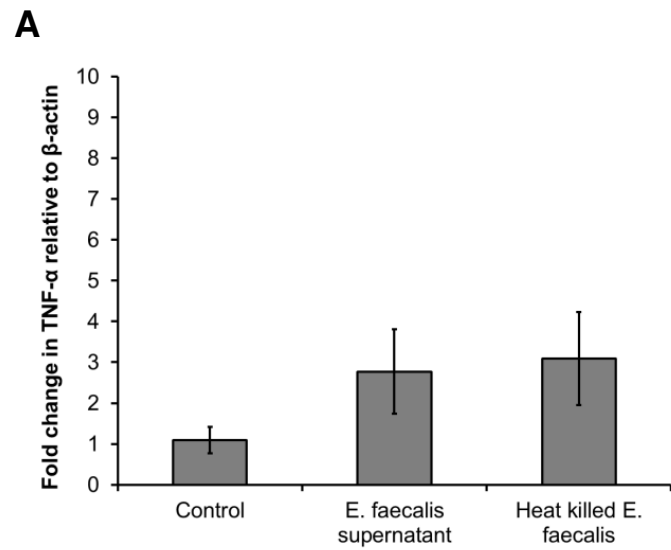


Table 1: Growth rates during the log phase of *S. anginosus* and *E. faecalis* alone and in combination at ratio of 50:50 and 90:10 respectively.

	<b>Average growth rate during log phase (CFUs/mL per hour)</b>	<b>Standard deviation</b>
<i>E. faecalis</i> (alone)	1.51	0.20
<i>S. anginosus</i> (alone)	2.00	0.25
<i>E. faecalis</i> (50:50)	1.62	0.10
<i>S. anginosus</i> (50:50)	1.53	0.14
<i>E. faecalis</i> (90:10)	1.98	0.12
<i>S. anginosus</i> (90:10)	1.57	0.12

Table 2: Primer sequences used for qPCR analysis

Gene	Primer sequence (5'-3')	Product length (Bp)	Melting temperature (°C)	Efficiency (%)	Source
Glyceraldehyde 3-phosphate dehydrogenase (GAPDH - NM_017008.4)	Forward – GCA AGA GAG AGG CCC TCA G Reverse – TGT GAG GGA GAT GCT CAG TG	74	61.0 59.4	106.37	(48)
Beta-actin ( $\beta$ -actin - NM_031144.3)	Forward – TGA AGA TCA AGA TCA TTG CTC CTC C Reverse – CTA GAA GCA TTT GCG GTG GAC GAT G	155	60.69 64.37	108.56	(49)
Hypoxanthine Phosphoribosyltransferase 1 (HPRT-1 - NM_012583.2)	Forward – TGT TTG TGT CAT CAG CGA AAG TG Reverse – ATT CAA CTT GCC GCT GTC TTT TA	66	60.24 59.43	91.71	(50)
Ribosomal Protein L13a (RPL13a - NM_173340.2)	Forward – GGA TCC CTC CAC CCT ATG ACA Reverse – CTG GTA CTT CCA CCC GAC CTC	131	61.8 63.7	99.99	(51)
18s ribosomal RNA (18s rRNA – V01270)	Forward – AAA CGG CTA CCA CAT CCA AG Reverse – TTG CCC TCC AAT GGA TCC T	159	57.3 56.7	90.22	(52)
Tumor necrosis factor alpha (TNF- $\alpha$ - NM_012675.3)	Forward – AAA TGG GCT CCC TCT CAT CAG TTC Reverse – TCT GCT TGG TGG TTT GCT ACG AC	111	62.7 62.4	90.28	(53)
Interleukin 1 beta (IL-1 $\beta$ - NM_031512.2)	Forward – ATG CCT CGT GCT GTC TGA CCC ATG TGA G Reverse – CCC AAG GCC ACA GGG ATT TTG TCG TTG C	135	70.06 70.16	94.80	